

Directed Flow of Identified Particles in Au + Au Collisions at $\sqrt{s_{NN}} = 200$ GeV at RHIC

L. Adamczyk,⁹ G. Agakishiev,¹⁹ M. M. Aggarwal,³⁰ Z. Ahammed,⁴⁸ A. V. Alakhverdyants,¹⁹ I. Alekseev,¹⁷ J. Alford,²⁰ B. D. Anderson,²⁰ C. D. Anson,²⁸ D. Arkhipkin,² G. S. Averichev,¹⁹ J. Balewski,²⁴ A. Banerjee,⁴⁸ Z. Barnovska,¹² D. R. Beavis,² R. Bellwied,⁴⁴ M. J. Betancourt,²⁴ R. R. Betts,⁸ A. Bhasin,¹⁸ A. K. Bhati,³⁰ H. Bichsel,⁵⁰ J. Bielcik,¹¹ J. Bielcikova,¹² L. C. Bland,² I. G. Bordyuzhin,¹⁷ W. Borowski,⁴¹ J. Bouchet,²⁰ A. V. Brandin,²⁷ S. G. Brovko,⁴ E. Bruna,⁵² S. Bueltmann,²⁹ I. Bunzarov,¹⁹ T. P. Burton,² J. Butterworth,³⁶ X. Z. Cai,⁴⁰ H. Caines,⁵² M. Calderón de la Barca Sánchez,⁴ D. Cebra,⁴ R. Cendejas,⁵ M. C. Cervantes,⁴² P. Chaloupka,¹² S. Chattopadhyay,⁴⁸ H. F. Chen,³⁸ J. H. Chen,⁴⁰ J. Y. Chen,⁷ L. Chen,⁷ J. Cheng,⁴⁵ M. Cherney,¹⁰ A. Chikanian,⁵² W. Christie,² P. Chung,¹² J. Chwastowski,⁹ M. J. M. Coddington,⁴² R. Corliss,²⁴ J. G. Cramer,⁵⁰ H. J. Crawford,³ X. Cui,³⁸ A. Davila Leyva,⁴³ L. C. De Silva,⁴⁴ R. R. Debebe,² T. G. Dedovich,¹⁹ J. Deng,³⁹ R. Derradi de Souza,⁶ S. Dhamija,¹⁶ L. Didenko,² F. Ding,⁴ P. Djawotho,⁴² X. Dong,²³ J. L. Drachenberg,⁴² J. E. Draper,⁴ C. M. Du,²² L. E. Dunkelberger,⁵ J. C. Dunlop,² L. G. Efimov,¹⁹ M. Elnimr,⁵¹ J. Engelage,³ G. Eppley,³⁶ L. Eun,²³ O. Evdokimov,⁸ R. Fatemi,²¹ J. Fedorisin,¹⁹ R. G. Fersch,²¹ P. Filip,¹⁹ E. Finch,⁵² Y. Fisyak,² C. A. Gagliardi,⁴² D. R. Gangadharan,²⁸ F. Geurts,³⁶ S. Gliske,¹ Y. N. Gorbunov,¹⁰ O. G. Grebenyuk,²³ D. Grosnick,⁴⁷ S. Gupta,¹⁸ W. Guryn,² B. Haag,⁴ O. Hajkova,¹¹ A. Hamed,⁴² L.-X. Han,⁴⁰ J. W. Harris,⁵² J. P. Hays-Wehle,²⁴ S. Heppelmann,³¹ A. Hirsch,³³ G. W. Hoffmann,⁴³ D. J. Hofman,⁸ S. Horvat,⁵² B. Huang,³⁸ H. Z. Huang,⁵ P. Huck,⁷ T. J. Humanic,²⁸ L. Huo,⁴² G. Igo,⁵ W. W. Jacobs,¹⁶ C. Jena,¹⁴ J. Joseph,²⁰ E. G. Judd,³ S. Kabana,⁴¹ K. Kang,⁴⁵ J. Kapitan,¹² K. Kauder,⁸ H. W. Ke,⁷ D. Keane,²⁰ A. Kechechyan,¹⁹ A. Kesich,⁴ D. Kettler,⁵⁰ D. P. Kikola,³³ J. Kiryluk,²³ A. Kisiel,⁴⁹ V. Kizka,¹⁹ S. R. Klein,²³ D. D. Koetke,⁴⁷ T. Kollegger,¹³ J. Konzer,³³ I. Koralt,²⁹ L. Koroleva,¹⁷ W. Korsch,²¹ L. Kotchenda,²⁷ P. Kravtsov,²⁷ K. Krueger,¹ L. Kumar,²⁰ M. A. C. Lamont,² J. M. Landgraf,² S. LaPointe,⁵¹ J. Lauret,² A. Lebedev,² R. Lednicki,¹⁹ J. H. Lee,² W. Leight,²⁴ M. J. LeVine,² C. Li,³⁸ L. Li,⁴³ W. Li,⁴⁰ X. Li,³³ X. Li,³⁹ Y. Li,⁴⁵ Z. M. Li,⁷ L. M. Lima,³⁷ M. A. Lisa,²⁸ F. Liu,⁷ T. Ljubicic,² W. J. Llope,³⁶ R. S. Longacre,² Y. Lu,³⁸ X. Luo,⁷ A. Luszczak,⁹ G. L. Ma,⁴⁰ Y. G. Ma,⁴⁰ D. P. Mahapatra,¹⁴ R. Majka,⁵² O. I. Mall,⁴ S. Margetis,²⁰ C. Markert,⁴³ H. Masui,²³ H. S. Matis,²³ D. McDonald,³⁶ T. S. McShane,¹⁰ S. Mioduszewski,⁴² M. K. Mitrovski,² Y. Mohammed,⁴² B. Mohanty,⁴⁸ B. Morozov,¹⁷ M. G. Munhoz,³⁷ M. K. Mustafa,³³ M. Naglis,²³ B. K. Nandi,¹⁵ Md. Nasim,⁴⁸ T. K. Nayak,⁴⁸ L. V. Nogach,³² G. Odyniec,²³ A. Ogawa,² K. Oh,³⁴ A. Ohlson,⁵² V. Okorokov,²⁷ E. W. Oldag,⁴³ R. A. N. Oliveira,³⁷ D. Olson,²³ M. Pachr,¹¹ B. S. Page,¹⁶ S. K. Pal,⁴⁸ Y. X. Pan,⁵ Y. Pandit,²⁰ Y. Panebratsev,¹⁹ T. Pawlak,⁴⁹ B. Pawlik,⁹ H. Pei,⁸ C. Perkins,³ W. Peryt,⁴⁹ P. Pile,² M. Planinic,⁵³ J. Pluta,⁴⁹ D. Plyku,²⁹ N. Poljak,⁵³ J. Porter,²³ A. M. Poskanzer,²³ C. B. Powell,²³ D. Prindle,⁵⁰ C. Pruneau,⁵¹ N. K. Pruthi,³⁰ M. Przybycien,⁹ P. R. Pujahari,¹⁵ J. Putschke,⁵¹ H. Qiu,²² R. Raniwala,³⁵ S. Raniwala,³⁵ R. L. Ray,⁴³ R. Redwine,²⁴ R. Reed,⁴ C. K. Riley,⁵² H. G. Ritter,²³ J. B. Roberts,³⁶ O. V. Rogachevskiy,¹⁹ J. L. Romero,⁴ L. Ruan,² J. Rusnak,¹² N. R. Sahoo,⁴⁸ I. Sakrejda,²³ S. Salur,²³ J. Sandweiss,⁵² E. Sangaline,⁴ A. Sarkar,¹⁵ J. Schambach,⁴³ R. P. Scharenberg,³³ A. M. Schmah,²³ N. Schmitz,²⁵ T. R. Schuster,¹³ J. Seele,²⁴ J. Seger,¹⁰ P. Seyboth,²⁵ N. Shah,⁵ E. Shahaliev,¹⁹ M. Shao,³⁸ B. Sharma,³⁰ M. Sharma,⁵¹ S. S. Shi,⁷ Q. Y. Shou,⁴⁰ E. P. Sichtermann,²³ R. N. Singaraju,⁴⁸ M. J. Skoby,³³ N. Smirnov,⁵² D. Solanki,³⁵ P. Sorensen,² U. G. deSouza,³⁷ H. M. Spinka,¹ B. Srivastava,³³ T. D. S. Stanislaus,⁴⁷ S. G. Steadman,²⁴ J. R. Stevens,¹⁶ R. Stock,¹³ M. Strikhanov,²⁷ B. Stringfellow,³³ A. A. P. Suaide,³⁷ M. C. Suarez,⁸ M. Sumera,¹² X. M. Sun,²³ Y. Sun,³⁸ Z. Sun,²² B. Surrow,²⁴ D. N. Svirida,¹⁷ T. J. M. Symons,²³ A. Szanto de Toledo,³⁷ J. Takahashi,⁶ A. H. Tang,² Z. Tang,³⁸ L. H. Tarini,⁵¹ T. Tarnowsky,²⁶ D. Thein,⁴³ J. H. Thomas,²³ J. Tian,⁴⁰ A. R. Timmins,⁴⁴ D. Tlusty,¹² M. Tokarev,¹⁹ T. A. Trainor,⁵⁰ S. Trentalange,⁵ R. E. Tribble,⁴² P. Tribedy,⁴⁸ B. A. Trzeciak,⁴⁹ O. D. Tsai,⁵ J. Turnau,⁹ T. Ullrich,² D. G. Underwood,¹ G. Van Buren,² G. van Nieuwenhuizen,²⁴ J. A. Vanfossen, Jr.,²⁰ R. Varma,¹⁵ G. M. S. Vasconcelos,⁶ F. Videbæk,² Y. P. Viyogi,⁴⁸ S. Vokal,¹⁹ S. A. Voloshin,⁵¹ A. Vossen,¹⁶ M. Wada,⁴³ F. Wang,³³ G. Wang,⁵ H. Wang,²⁶ J. S. Wang,²² Q. Wang,³³ X. L. Wang,³⁸ Y. Wang,⁴⁵ G. Webb,²¹ J. C. Webb,² G. D. Westfall,²⁶ C. Whitten, Jr.,⁵ H. Wieman,²³ S. W. Wissink,¹⁶ R. Witt,⁴⁶ W. Witzke,²¹ Y. F. Wu,⁷ Z. Xiao,⁴⁵ W. Xie,³³ K. Xin,³⁶ H. Xu,²² N. Xu,²³ Q. H. Xu,³⁹ W. Xu,⁵ Y. Xu,³⁸ Z. Xu,² L. Xue,⁴⁰ Y. Yang,²² Y. Yang,⁷ P. Yepes,³⁶ Y. Yi,³³ K. Yip,² I.-K. Yoo,³⁴ M. Zawisza,⁴⁹ H. Zbroszczyk,⁴⁹ J. B. Zhang,⁷ S. Zhang,⁴⁰ W. M. Zhang,²⁰ X. P. Zhang,⁴⁵ Y. Zhang,³⁸ Z. P. Zhang,³⁸ F. Zhao,⁵ J. Zhao,⁴⁰ C. Zhong,⁴⁰ X. Zhu,⁴⁵ Y. H. Zhu,⁴⁰ and Y. Zoukarnieva¹⁹

(STAR Collaboration)

¹Argonne National Laboratory, Argonne, Illinois 60439, USA
²Brookhaven National Laboratory, Upton, New York 11973, USA

- ³University of California, Berkeley, California 94720, USA
⁴University of California, Davis, California 95616, USA
⁵University of California, Los Angeles, California 90095, USA
⁶Universidade Estadual de Campinas, Sao Paulo, Brazil
⁷Central China Normal University (HZNU), Wuhan 430079, China
⁸University of Illinois at Chicago, Chicago, Illinois 60607, USA
⁹Krakow University of Technology, Crakow, Poland
¹⁰Creighton University, Omaha, Nebraska 68178, USA
¹¹Czech Technical University in Prague, FNSPE, Prague, 115 19, Czech Republic
¹²Nuclear Physics Institute AS CR, 250 68 Řež/Prague, Czech Republic
¹³University of Frankfurt, Frankfurt, Germany
¹⁴Institute of Physics, Bhubaneswar 751005, India
¹⁵Indian Institute of Technology, Mumbai, India
¹⁶Indiana University, Bloomington, Indiana 47408, USA
¹⁷Alkhanov Institute for Theoretical and Experimental Physics, Moscow, Russia
¹⁸University of Jammu, Jammu 180001, India
¹⁹Joint Institute for Nuclear Research, Dubna, 141 980, Russia
²⁰Kent State University, Kent, Ohio 44242, USA
²¹University of Kentucky, Lexington, Kentucky, 40506-0055, USA
²²Institute of Modern Physics, Lanzhou, China
²³Lawrence Berkeley National Laboratory, Berkeley, California 94720, USA
²⁴Massachusetts Institute of Technology, Cambridge, Massachusetts 02139-4307, USA
²⁵Max-Planck-Institut für Physik, Munich, Germany
²⁶Michigan State University, East Lansing, Michigan 48824, USA
²⁷Moscow Engineering Physics Institute, Moscow Russia
²⁸Ohio State University, Columbus, Ohio 43210, USA
²⁹Old Dominion University, Norfolk, Virginia 23529, USA
³⁰Panjab University, Chandigarh 160014, India
³¹Pennsylvania State University, University Park, Pennsylvania 16802, USA
³²Institute of High Energy Physics, Protvino, Russia
³³Purdue University, West Lafayette, Indiana 47907, USA
³⁴Pusan National University, Pusan, Republic of Korea
³⁵University of Rajasthan, Jaipur 302004, India
³⁶Rice University, Houston, Texas 77251, USA
³⁷Universidade de Sao Paulo, Sao Paulo, Brazil
³⁸University of Science & Technology of China, Hefei 230026, China
³⁹Shandong University, Jinan, Shandong 250100, China
⁴⁰Shanghai Institute of Applied Physics, Shanghai 201800, China
⁴¹SUBATECH, Nantes, France
⁴²Texas A&M University, College Station, Texas 77843, USA
⁴³University of Texas, Austin, Texas 78712, USA
⁴⁴University of Houston, Houston, Texas 77204, USA
⁴⁵Tsinghua University, Beijing 100084, China
⁴⁶United States Naval Academy, Annapolis, Maryland 21402, USA
⁴⁷Valparaiso University, Valparaiso, Indiana 46383, USA
⁴⁸Variable Energy Cyclotron Centre, Kolkata 700064, India
⁴⁹Warsaw University of Technology, Warsaw, Poland
⁵⁰University of Washington, Seattle, Washington 98195, USA
⁵¹Wayne State University, Detroit, Michigan 48201, USA
⁵²Yale University, New Haven, Connecticut 06520, USA
⁵³University of Zagreb, Zagreb, HR-10002, Croatia

(Received 16 December 2011; published 15 May 2012)

STAR's measurements of directed flow (v_1) around midrapidity for π^\pm , K^\pm , K_S^0 , p , and \bar{p} in Au + Au collisions at $\sqrt{s_{NN}} = 200$ GeV are presented. A negative $v_1(y)$ slope is observed for most of produced particles (π^\pm , K^\pm , K_S^0 , and \bar{p}). In 5%–30% central collisions, a sizable difference is present between the $v_1(y)$ slope of protons and antiprotons, with the former being consistent with zero within errors. The v_1 excitation function is presented. Comparisons to model calculations (RQMD, UrQMD, AMPT, QGSM with parton recombination, and a hydrodynamics model with a tilted source) are made. For those models which have calculations of v_1 for both pions and protons, none of them can describe $v_1(y)$ for

pions and protons simultaneously. The hydrodynamics model with a tilted source as currently implemented cannot explain the centrality dependence of the difference between the $v_1(y)$ slopes of protons and antiprotons.

DOI: 10.1103/PhysRevLett.108.202301

PACS numbers: 25.75.Ld

The BNL Relativistic Heavy Ion Collider (RHIC) was built to study a new form of matter known as the quark-gluon plasma (QGP) [1], which existed in the Universe shortly after the big bang. At RHIC, two nuclei are collided at near light speed, and the collision produces thousands of particles due to the significant energy deposited. The collective motion of the produced particles can be characterized [2] by Fourier coefficients,

$$v_n = \langle \cos n(\phi - \psi) \rangle, \quad (1)$$

where n denotes the harmonic, ϕ and ψ denote the azimuthal angle of an outgoing particle and reaction plane, respectively. The reaction plane is defined by the collision axis and the line connecting the centers of two nuclei. Thus far, five of these coefficients have been measured and found to be nonzero at RHIC [3]. They are directed flow v_1 , elliptic flow v_2 , triangular flow v_3 , the fourth-order harmonic flow v_4 , and the sixth-order harmonic flow v_6 . This Letter will focus on the directed flow, the first Fourier coefficient.

Directed flow describes the sideward motion of produced particles in ultrarelativistic nuclear collisions. It is believed to be generated during the nuclear passage time before the thermalization happens; thus, it carries early information from the collision [4–7]. The shape of directed flow at midrapidity may be modified by the collective expansion and reveal a signature of a possible phase transition from normal nuclear matter to a QGP [8–10]. It is argued that directed flow, as an odd function of rapidity (y), may exhibit a small slope (flatness) at midrapidity due to a strong expansion of the fireball being tilted away from the collision axis. Such tilted expansion gives rise to antiflow [8] or a third-flow [9] component (not the third flow harmonic). The antiflow (or the third-flow component) is perpendicular to the source surface, and is in the opposite direction to the bouncing-off motion of nucleons. If the tilted expansion is strong enough, it can even overcome the bouncing-off motion and results in a negative $v_1(y)$ slope at midrapidity, potentially producing a wiggly structure in $v_1(y)$. Note that although calculations [8,9] for both antiflow and third-flow component are made for collisions at Super Proton Synchrotron (SPS) energies where the first-order phase transition to a QGP is believed to be the most relevant [10], the direct cause of the negative slope is the strong, tilted expansion, which is also important at RHIC's top energies. Indeed, hydrodynamic calculations [11] for Au + Au collisions at $\sqrt{s_{NN}} = 200$ GeV with a tilted source as the initial condition can give a similar negative $v_1(y)$ slope as that found in data. A wiggly structure is also

seen in the relativistic quantum molecular dynamics (RQMD) model [12], and it is attributed to baryon stopping together with a positive space-momentum correlation. In this picture, no phase transition is needed, and pions and nucleons flow in opposite directions. To distinguish between baryon stopping and antiflow, it is desirable to measure the $v_1(y)$ for identified particles and compare the sign of their slopes at midrapidity. In particular, the observation of a centrality dependence of proton $v_1(y)$ may reveal the character of a possible first-order phase transition [10]. It is expected that in very peripheral collisions, the bouncing-off motion dominates over the entire rapidity range, and protons at midrapidity flow in the same direction as spectators. In midcentral collisions, if there is a phase transition, the proton $v_1(y)$ slope at midrapidity may change sign and become negative. Eventually the slope diminishes in central collisions due to the symmetry of the collisions.

The E895 Collaboration has shown that at low energies K_S^0 has a negative $v_1(y)$ slope around midrapidity [13], while Λ and protons have positive slopes [14]. This is explained by a repulsive kaon-nucleon potential and an attractive Λ -nucleon potential. The NA49 Collaboration [15] has measured v_1 for pions and protons, and a negative $v_1(y)$ slope is observed by the standard event plane method. The three-particle correlation method $v_1\{3\}$ [16], which is believed to be less sensitive to nonflow effects, gives a negative slope too, but with a larger statistical error. The nonflow effects are correlations among particles that are not related to the reaction plane, including the quantum Hanbury Brown–Twiss correlation [17], resonance decays [18], and so on. At top RHIC energies, v_1 has been studied mostly for charged particles by both the STAR and the PHOBOS Collaborations [19–22]. It is found that v_1 in the forward region follows the limiting fragmentation hypothesis [23], and v_1 as a function of pseudorapidity (η) depends only on the incident energy, but not on the size of the colliding system at a given centrality. Such system size independence of v_1 can be explained by the hydrodynamic calculation with a tilted initial condition [11]. The systematic study of v_1 for identified particles at RHIC did not begin until recently because it is more challenging for two reasons: (1) v_1 for some identified particles (for example, protons) is much smaller than that of all charged particles and (2) more statistics are needed to determine v_1 for identified particles other than pions.

Fifty-four million events from Au + Au collisions at $\sqrt{s_{NN}} = 200$ GeV have been used in this study, all taken by a minimum-bias trigger with the STAR detector during RHIC's seventh run in year 2007. The main trigger detector

used is the vertex position detector (VPD) [24]. The centrality definition of an event was based on the number of charged tracks in the time projection chamber (TPC) [25] with track quality cuts: $|\eta| < 0.5$, a distance of closest approach (DCA) to the vertex less than 3 cm, and 10 or more fit points. In the analysis, events are required to have the vertex z within 30 cm from the center of the TPC, and additional weight is assigned to each event in the analysis, accounting for the nonuniform VPD trigger efficiency in the vertex z direction for different centrality classes. The event plane angle is determined from the sideward deflection of spectator neutrons measured by STAR's shower maximum detector inside the zero degree calorimeters (ZDC-SMDs). Such sideward deflection of spectator neutrons is expected to happen in the reaction plane rather than participant plane, since the ZDC-SMDs are located close to beam rapidity. Being 6 units in η away from midrapidity, ZDC-SMDs also allow a measurement of v_1 with minimal contribution from nonflow correlations. The description of measuring v_1 using the ZDC-SMDs event plane can be found in [21]. Particle identification (PID) of charged particles is achieved by measuring ionization energy loss (dE/dx) inside STAR's TPC, together with the measurement of the momentum (p) via TPC tracking. Track quality cuts are the same as used in [26]. In addition, the transverse momentum p_T for protons is required to be larger than 400 MeV/ c , and DCA is required to be less than 1 cm in order to avoid including background protons which are from knockout/nuclear interactions of pions with inner detector material. The same cuts are applied to antiprotons as well to ensure a fair comparison with protons. The high end of the p_T cut is 1 GeV/ c , where protons and pions have the same energy loss in the TPC and thus become indistinguishable. For pions and kaons, the p_T range is 0.15–0.75 GeV/ c and 0.2–0.6 GeV/ c , respectively. K_S^0 ($\rightarrow \pi^+ \pi^-$) are topologically reconstructed by their charged daughter tracks inside the TPC [27].

Results presented in the following figures contain only statistical errors. Results for pions, protons, and antiprotons are not corrected for the feeddown from weak decay particles. The major systematic error in determining the slope of $v_1(y)$ for identified particles is from the particle misidentification, which was evaluated by varying the dE/dx cut. Another systematic error comes from the non-uniform p_T acceptance, as $v_1(y)$ is obtained by integrating v_1 over the p_T acceptance, which itself depends on the rapidity. This effect is non-negligible for protons and antiprotons at large rapidity. It is estimated by taking the difference between slopes fitted with points integrated with p_T acceptance at midrapidity and at large rapidity. In addition, some of the observed protons have originated from interactions between the produced particles and the detector material, and such effect has also been taken into consideration. The total systematic uncertainty is obtained by adding uncertainties mentioned above in quadrature.

There are also common systematic errors that should be applied to all particles: the uncertainty due to the first-order event plane determination, which was estimated to be $\sim 10\%$ (relative error) [21], and the uncertainty due to centrality selection, which was estimated to be $\sim 4\%$ (relative error) by comparing our charged $v_1(\eta)$ slope to that from the RHIC run in 2004. Other systematic errors have been evaluated to be negligible.

In Fig. 1, $v_1(y)$ of π^\pm , K^\pm , K_S^0 , p , and \bar{p} are presented for centrality 10%–70%. Following convention, the sign of spectator v_1 in the forward region is chosen to be positive, to which the measured sign of v_1 for particles of interest is only relative. Fitting with a linear function, the slopes are $-0.15 \pm 0.05(\text{stat}) \pm 0.08(\text{syst})(\%)$ for the protons, $-0.46 \pm 0.06(\text{stat}) \pm 0.04(\text{syst})(\%)$ for the anti-protons, $-0.27 \pm 0.01(\text{stat}) \pm 0.01(\text{syst})(\%)$ for the pions, $-0.02 \pm 0.11(\text{stat}) \pm 0.04(\text{syst})(\%)$ for the kaons and $-0.17 \pm 0.02(\text{stat}) \pm 0.04(\text{syst})(\%)$ for the K_S^0 . The relative 10% common systematic error for all particles is not listed here. The $v_1(y)$ slope for the produced particle types (π^\pm , K^\pm , K_S^0 , and \bar{p}) are mostly found to be negative at midrapidity, which is consistent with the antiflow picture. In particular, kaons are less sensitive to shadowing effects due to the small kaon-nucleon cross section, yet they show a negative slope. This is again consistent with the antiflow picture. Interestingly, $v_1(y)$ for protons exhibits a clearly flatter shape than that for antiprotons. While mass may contribute to the difference in slope between pions and protons or antiprotons, it cannot explain the difference in slope observed for antiprotons and protons. Indeed, the observed v_1 for protons is a convolution of directed flow of produced protons with that of transported protons (from the original projectile and target nuclei), so the flatness of inclusive proton $v_1(y)$ around midrapidity could be explained by the negative flow of produced protons being compensated by the positive flow of protons transported from spectator rapidity, as a feature expected in the anti-flow picture.

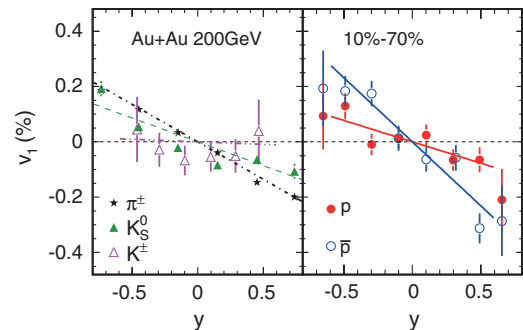


FIG. 1 (color). v_1 for π^\pm , K^\pm , K_S^0 (left panel), p and \bar{p} (right panel) as a function of rapidity for 10%–70% Au + Au collisions at $\sqrt{s_{NN}} = 200$ GeV. The lines present the linear fit to the π^\pm , K^\pm , K_S^0 , p , and \bar{p} 's $v_1(y)$, respectively. Data points around $y = 0.29$ are slightly shifted horizontally to avoid overlapping.

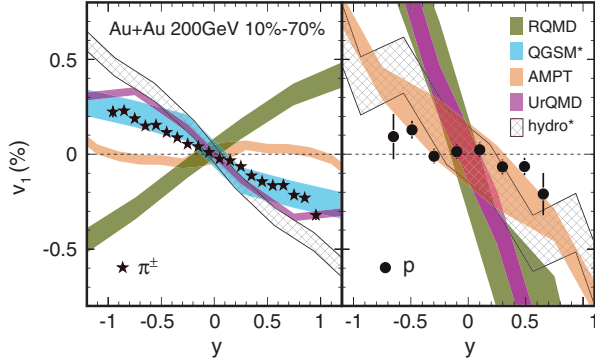


FIG. 2 (color). Model calculations of pion (left panel) and proton (right panel) $v_1(y)$ for 10%–70% Au + Au collisions at $\sqrt{s_{NN}} = 200$ GeV. The QGSM* model presents the basic quark-gluon string model with parton recombination [30]. The hydro* model presents the hydrodynamic expansion from a tilted source [11].

In Fig. 2, pion and proton $v_1(y)$ are plotted together with five model calculations, namely, RQMD [12], UrQMD [28], AMPT [29], QGSM with parton recombination [30], and slopes from an ideal hydrodynamic calculation with a tilted source [11]. The model calculations are performed in the same p_T acceptance and centrality as the data. The RQMD and AMPT model calculations predict the wrong sign and wrong magnitude of pion $v_1(y)$, respectively, while the RQMD and the UrQMD model calculations predict the wrong magnitude of proton $v_1(y)$. For models other than QGSM, which has the calculation only for pions, none of them can describe $v_1(y)$ for pions and protons simultaneously.

In Fig. 3, the slope of $v_1(y)$ at midrapidity is presented as a function of centrality for protons, antiprotons, and charged pions. In general, the magnitude of the $v_1(y)$ slope converges to zero as expected for most central collisions. Proton and antiproton $v_1(y)$ slopes are more or less consistent in 30%–80% centrality range but diverge in 5%–30% centrality. In addition, two observations are noteworthy: (i) the hydrodynamic model with tilted source (which is a characteristic of antiflow) as currently implemented does not predict the

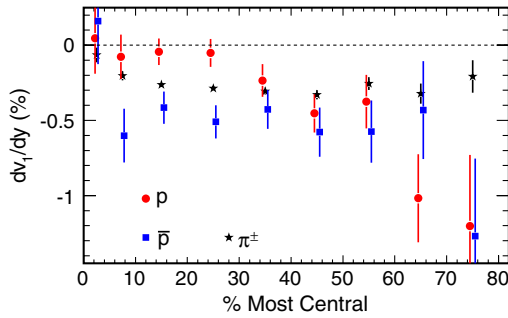


FIG. 3 (color online). Charged pions (solid stars), protons (solid circles), and antiprotons (solid squares) $v_1(y)$ slope (dv_1/dy) at midrapidity as a function of centrality for Au + Au collisions at $\sqrt{s_{NN}} = 200$ GeV.

difference in $v_1(y)$ between particle species [31]; (ii) if the difference between v_1 of protons and antiprotons is caused by antiflow alone, then such difference is expected to be accompanied by strongly negative v_1 slopes. In data, the large difference between proton and antiproton v_1 slopes is seen in the 5%–30% centrality range, while strongly negative v_1 slopes are found for protons, antiprotons, and charged pions in a different centrality range (30%–80%). Both observations suggest that additional mechanisms than that assumed in [11,31] are needed to explain the centrality dependence of the difference between the $v_1(y)$ slopes of protons and antiprotons.

The excitation function of proton $v_1(y')$ slope $F (= dv_1/dy'$ at midrapidity) is presented in Fig. 4. Values for F are extracted via a polynomial fit of the form $Fy' + Cy'^3$, where $y' = y/y_{\text{beam}}$ for which spectators are normalized at ± 1 . The proton $v_1(y')$ slope decreases rapidly with increasing energy, reaching zero around $\sqrt{s_{NN}} = 9$ GeV. Its sign changes to negative as shown by the data point at $\sqrt{s_{NN}} = 17$ GeV, measured by the NA49 experiment [15]. A similar trend has been observed at low energies with a slightly different quantity $d\langle p_x \rangle / dy'$ [32,33]. The energy dependence of the $v_1(y')$ slope for protons is driven by two factors: (i) the increase in the number of produced protons over transported protons with increasing energy, and (ii) the v_1 of both produced and transported protons at different energies. The negative $v_1(y')$ slope for protons around midrapidity at SPS energies cannot be explained by transport model calculations like UrQMD [34] and AMPT [29], but is predicted by hydrodynamics calculations [8,9]. The present data indicate that the proton v_1 slope remains close to zero at $\sqrt{s_{NN}} = 200$ GeV as observed at $\sqrt{s_{NN}} = 9$ GeV and $\sqrt{s_{NN}} = 17$ GeV heavy ion collisions. Our measurement offers a unique check of the validity of a tilted expansion at RHIC top energy.

In summary, STAR's measurements of directed flow of pions, kaons, protons, and antiprotons for Au + Au collisions at $\sqrt{s_{NN}} = 200$ GeV are presented. In the range of 10%–70% central collisions, $v_1(y)$ slopes of pions, kaons (K_S^0), and antiprotons are found to be mostly negative at

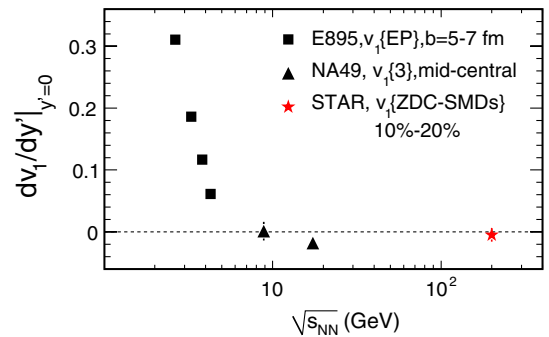


FIG. 4 (color online). Proton $v_1(y')$ slope (dv_1/dy') at midrapidity as a function of center of mass collision energy, where $y' = y/y_{\text{beam}}$.

midrapidity. In 5%–30% central collisions, a sizable difference is present between the $v_1(y)$ slope of protons and antiprotons, with the former being consistent with zero within errors. Comparison to models (RQMD, UrQMD, AMPT, QGSM with parton recombination, and hydrodynamics with a tilted source) is made. Putting aside the QGSM model, which has the calculation only for pions, none of the other models explored can describe $v_1(y)$ for pions and protons simultaneously. Additional mechanisms than that assumed in the hydrodynamics model with a tilted source [11,31] are needed to explain the centrality dependence of the difference between the $v_1(y)$ slopes of protons and antiprotons. Our measurement indicates that the proton's $v_1(y)$ slope remains close to zero for Au + Au collisions at $\sqrt{s_{NN}} = 200$ GeV. These new measurements on the particle species and centrality dependence of $v_1(y)$ provides a check for the validity of a tilted expansion at RHIC top energy.

We thank the RHIC Operations Group and RCF at BNL, the NERSC Center at LBNL and the Open Science Grid consortium for providing resources and support. This work was supported in part by the Offices of NP and HEP within the U.S. DOE Office of Science, the U.S. NSF, the Sloan Foundation; the DFG cluster of excellence “Origin and Structure of the Universe” of Germany; CNRS/IN2P3, FAPESP CNPq of Brazil; Ministry of Education and Science of the Russian Federation; NNSFC, CAS, MoST, and MoE of China; GA and MSMT of the Czech Republic; FOM and NWO of the Netherlands; DAE, DST, and CSIR of India; Polish Ministry of Science and Higher Education; Korea Research Foundation; Ministry of Science, Education, and Sports of the Republic of Croatia; and RosAtom of Russia.

-
- [1] I. Arsenej *et al.* (BRAHMS Collaboration), *Nucl. Phys.* **A757**, 1 (2005); K. Adcox *et al.* (PHENIX Collaboration), *Nucl. Phys.* **A757**, 184 (2005); B. B. Back *et al.* (PHOBOS Collaboration), *Nucl. Phys.* **A757**, 28 (2005); J. Adams *et al.* (STAR Collaboration), *Nucl. Phys.* **A757**, 102 (2005).
- [2] A. M. Poskanzer and S. A. Voloshin, *Phys. Rev. C* **58**, 1671 (1998).
- [3] S. Voloshin, A. Poskanzer, and R. Snellings, in *Relativistic Heavy Ion Physics*, edited by R. Stock (Springer-Verlag, Berlin, 2010), Vol. 23.
- [4] E. Schnedermann and U. Heinz, *Phys. Rev. Lett.* **69**, 2908 (1992).
- [5] D. E. Kahana, D. Keane, Y. Pang, T. Schlagel, and S. Wang, *Phys. Rev. Lett.* **74**, 4404 (1995).
- [6] J. Barrette *et al.* (E877 Collaboration), *Phys. Rev. Lett.* **73**, 2532 (1994).
- [7] I. G. Bearden *et al.* (NA44 Collaboration), *Phys. Rev. Lett.* **78**, 2080 (1997).
- [8] J. Brachmann, S. Soff, A. Dumitru, H. Stöcker, J. A. Maruhn, W. Greiner, L. V. Bravina, and D. H. Rischke, *Phys. Rev. C* **61**, 024909 (2000).
- [9] L. P. Csernai and D. Röhrich, *Phys. Lett. B* **458**, 454 (1999).
- [10] H. Stöcker, *Nucl. Phys.* **A750**, 121 (2005).
- [11] P. Božek and I. Wyskiel, *Phys. Rev. C* **81**, 054902 (2010).
- [12] R. J. M. Snellings, H. Sorge, S. A. Voloshin, F. Q. Wang, and N. Xu, *Phys. Rev. Lett.* **84**, 2803 (2000).
- [13] P. Chung *et al.* (E895 Collaboration), *Phys. Rev. Lett.* **85**, 940 (2000).
- [14] P. Chung *et al.* (E895 Collaboration), *Phys. Rev. Lett.* **86**, 2533 (2001).
- [15] C. Alt *et al.* (NA49 Collaboration), *Phys. Rev. C* **68**, 034903 (2003).
- [16] N. Borghini, P. M. Dinh, and J.-Y. Ollitrault, *Phys. Rev. C* **66**, 014905 (2002).
- [17] P. M. Dinh, N. Borghini, and J.-Y. Ollitrault, *Phys. Lett. B* **477**, 51 (2000).
- [18] N. Borghini, P. M. Dinh, and J.-Y. Ollitrault, *Phys. Rev. C* **62**, 034902 (2000).
- [19] J. Adams *et al.* (STAR Collaboration), *Phys. Rev. Lett.* **92**, 062301 (2004).
- [20] B. B. Back *et al.* (PHOBOS Collaboration), *Phys. Rev. Lett.* **97**, 012301 (2006).
- [21] J. Adams *et al.* (STAR Collaboration), *Phys. Rev. C* **73**, 034903 (2006).
- [22] B. I. Abelev *et al.* (STAR Collaboration), *Phys. Rev. Lett.* **101**, 252301 (2008).
- [23] J. Benecke, T. T. Chou, C. N. Yang, and E. Yen, *Phys. Rev.* **188**, 2159 (1969).
- [24] W. J. Llope *et al.*, *Nucl. Instrum. Methods Phys. Res., Sect. A* **522**, 252 (2004).
- [25] M. Anderson *et al.*, *Nucl. Instrum. Methods Phys. Res., Sect. A* **499**, 659 (2003).
- [26] J. Adams *et al.* (STAR Collaboration), *Phys. Rev. C* **72**, 014904 (2005).
- [27] C. Adler *et al.* (STAR Collaboration), *Phys. Rev. Lett.* **89**, 132301 (2002); J. Adams *et al.* (STAR Collaboration), *Phys. Rev. Lett.* **92**, 052302 (2004).
- [28] M. Bleicher and H. Stöcker, *Phys. Lett. B* **526**, 309 (2002).
- [29] J. Y. Chen, J. X. Zuo, X. Z. Cai, F. Liu, Y. G. Ma, and A. H. Tang, *Phys. Rev. C* **81**, 014904 (2010).
- [30] J. Bleibel, G. Burau, A. Faessler, and C. Fuchs, *Phys. Rev. C* **76**, 024912 (2007).
- [31] P. Božek (private communication).
- [32] H. Liu *et al.* (E895 Collaboration), *Phys. Rev. Lett.* **84**, 5488 (2000).
- [33] J. Barrette *et al.* (E877 Collaboration), *Phys. Rev. C* **56**, 3254 (1997); *Phys. Rev. C* **55**, 1420 (1997).
- [34] H. Petersen, Q. Li, X. Zhu, and M. Bleicher, *Phys. Rev. C* **74**, 064908 (2006).